A Front End Power-Factor-Corrected Converter fed Two Stage Battery Charger for Electric Vehicles*

Deepa M.U. Author[1] and Bindu G.R. Author[2]

Abstract— The effectiveness and efficiency of the method adopted for battery chargers with low input current distortion and better power factor are demanding for Electric Vehicles (EVs). On-Board-Charger (OBC) consists of two stage converters which includes the front end Power Factor Corrected (PFC) stage followed by a DC-DC converter. This paper presents a front end power factor corrected on-board battery charger for EVs. Bridgeless boost converter topology with less number of switches is selected as the PFC stage for battery charger and it is compared with other bridgeless topologies. Front end PFC converter followed by LLC resonant DC-DC converter is used here to develop the battery charger. A 48 V, 24Ah Li-ion battery pack is used as energy storage to drive EV and its charging through the proposed converter scheme is analysed using MATLAB/SIMULINK. The simulation results show the effectiveness of the proposed scheme.

Index Terms— Power Factor Correction, Bridgeless Converter, DC-DC Converter, On-Board Battery Charger, Electric Vehicle

I. INTRODUCTION

The environmental pollution due to combustion of fossil fuels and the rising crisis of petroleum fuels have led to the reduction in the dependence of conventional internal combustion engines. The electrification of automotive sector empowers sustainable energy sources and mitigates noise and air pollution. Electric Vehicles (EVs) are more competent option for transportation instead of conventional internal combustion engine. Because of the high energy density Li-ion batteries are used for energy storage in EVs. An intensive research has been carried out in the area of battery management, battery life, extension of driving range and charging infrastructure. The batteries use on board charger integrated into the vehicle for its charging. Single phase or three phase AC supply is given as the input to the on board battery charger. Power charging station of EV batteries can be classified as three configurations such as Level 1, Level 2 and Level 3 charger. Level 1 charger with single phase AC input is used in short distance EVs such as e-rickshaw, e-bikes and golfcarts [1].

These on-board battery charger consists of either a single stage converter with diode bridge rectifier cascaded with a non-isolated or isolated DC-DC converter stage which meets both input side and the output battery side requirements or a front end PFC converter which meets supply side requirements and followed by a DC-DC converter to meet the requirements of battery side. AC-DC conversion is done by diode bridge rectifier with capacitor filter which draws a non-sinusoidal current with high Total Harmonic Distortion (THD) and poor power factor (pf). In Conventional chargers, a diode bridge rectifier followed by boost converter topology employs PFC and which improves the input power factor and reduce THD [2]. Buck, boost and buck boost derived topologies are used to improve the performance in different power levels of operation [3]-[5].

Front end bridgeless converter configurations have also been proposed in PFC converters because of its simple design, less number of switches and high efficiency [6]. It has the additional advantage that it eliminates the front end diode bridge rectifier and possible to add interleaved operation to improve the output voltage[7]-[8]. This paper mainly focuses on the problems related to the power quality issues in EV charging infrastructure, specifically, PFC converter in the input AC-supply distribution network [9].

Second stage of an OBC is a DC-DC converter which provides galvanic isolation and required voltage for charging of battery. Resonant power converters are operating as DC-DC converter with high switching frequency and offers lower switching losses. Pulse frequency modulated gate signals instead of pulse width modulated signals are applied to the switches of LLC resonant converter to regulate the DC output voltage of the converter[10]-[11]. LLC resonant converter topology has the advantages like zero voltage switching, galvanic isolation and high power density. Output voltage of the LLC resonant converter can be regulated for a wide range of input voltage and load current with small variations in switching frequency[12]-[13]. Hence LLC resonant converter topology is adopted as the second stage in this paper for OBC scheme.

This paper analyses the performance in terms of power factor and THD of front end PFC converter of OBC used in EVs. The performance of on-board battery charger is analysed using a MATLAB/SIMULINK environment. Section II deals with the different bridgeless configurations. Section III presents the modes of operation of OBC used in EVs. Section IV deals with the design aspects of two stage on-board battery charger. Section V includes the performance analysis by simulation and comparison of bridgeless topologies for front end PFC converter based on power factor and THD. Section VI concludes the paper based on the results and performance analysis.

II. BRIDGELESS TOPOLOGIES FOR FRONT END PFC OF BATTERY CHARGER

The basic architecture of two stage on board battery charger is given in Fig.1. Front end bridge rectifier operates as a uncontrolled rectifier to convert input AC voltage to unregulated DC output voltage and Non-isolated DC-DC converter cascaded to bridge rectifier serves the function of a PFC stage. Second stage is an isolated DC-DC converter which controls the output voltage to meet the battery requirement. The efficiency of PFC converter can be improved by bridgeless configurations. The various types of bridgeless configurations are discussed here.
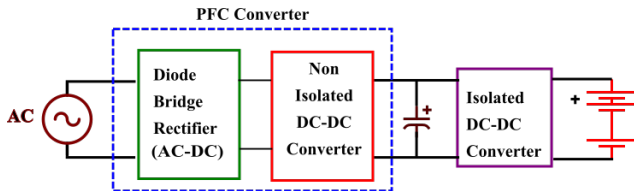

Fig. 1.   Block diagram of two stage OBC for EVs

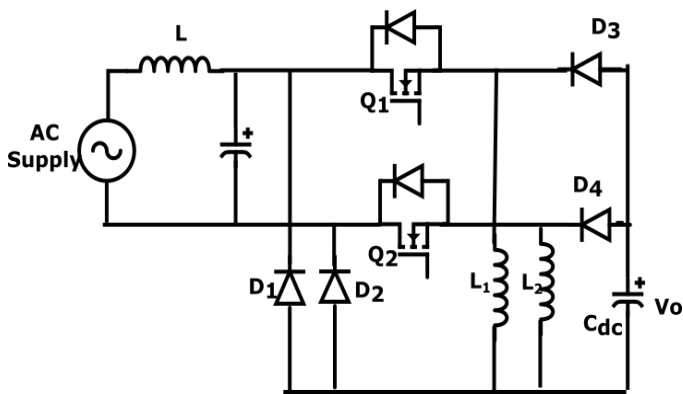### A. Bridgeless Buck boost Converter

Fig. 2.   Bridgeless Buck Boost Topology

Buck boost converter derived topology has the advantage that it can be used for wide range of output application with low distortion of output current. The bridgeless buck-boost topology is shown in Fig.2. It is a combination of two single-switch buck-boost converters, with each one operating over a half-cycle of the input sinusoidal voltage. During positive half cycle inductor L_1 charges through Q_1 and diode D_1 and it discharges through D_3. Similarly L_2 charges through Q_2 and diode D_2 and it discharges through D_4. It can operate in continuous conduction mode or discontinuous conduction mode. Based on it number of sensors vary. Discontinuous conduction mode needs less number of sensors and hence it is preferred for low power applications.

B. Bridgeless LUO Converter

Fig.3 shows the circuit diagram of bridgeless Luo converter. Two different switches operate in each half cycle to obtain bridgeless configuration. During positive half cycle of
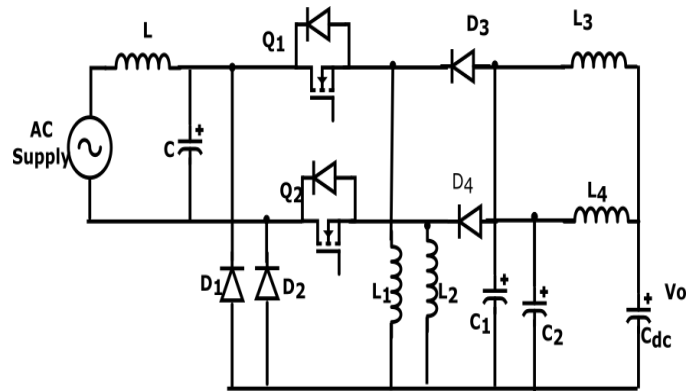

Fig. 3.   Bridgeless Luo Converter

supply voltage, switch Q_1 , Diodes D_1 and D_3 and inductor L_1 and L_3 are operating. Similarly for the negative half supply switch Q_2 , Diodes D_2 and D_4 and inductor L_2 and L_4 are operating. Input inductor current is in discontinuous in nature to operate as a power factor preregulator.

C. Bridgeless Dual boost Converter

Fig.4 shows the schematic diagram of front end AC-DC bridgeless boost converter. Q_1 and Q_2 are switched during the positive and negative half-cycles of the single phase input AC voltage and inductor charges through it. During the positive half cycle, boost inductor charges when PWM signals are applied to the gates of switches Q_1 and Q_2. The stored energy in the inductor discharges to the DC link capacitor through the diodes D_1 and body diode Q_2 . Similarly, during the negative half cycle, PWM signals are applied to the gates of switches Q_1 and Q_2, boost inductor charges in the opposite direction. Boost inductor discharges through D_2 and body diode Q_1. Here similar gate signals are applied to both switches. High operating efficiency can be attained with this converter topology upto 2kW and above that bridgeless interleaved boost converter shown in Fig.5 to be used.
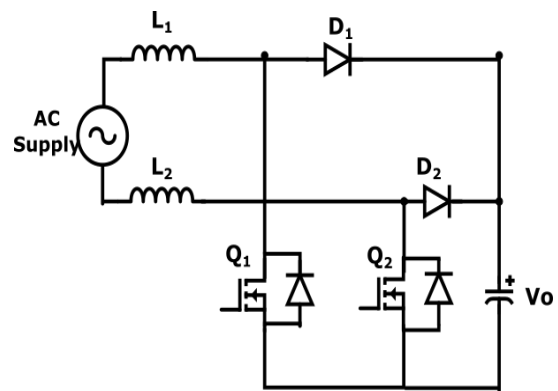

Fig. 4.   Bridgeless boost converter

D. Bridgeless Interleaved boost Converter

Converters are connected in parallel to obtain interleaved topology. Bridgeless interleaved boost converter is shown in

TABLE I

COMPARISON BETWEEN FRONT END PFC TOPOLOGIES

Method	Bridgeless Topology	No. of switches	No. of diodes	No.of Inductors	power rating	cost
Boost Converter	No	1	5	1		low
Bridgeless buck boost	Yes	2	4	2	Upto 600W	medium
Bridgeless Luo	Yes	2	4	4	Upto 800W	medium
Bridgeless Boost	Yes	2	2	2	upto 1.5kW	low
Bridgeless Interleaved boost	Yes	4	4	4	upto 3.5kW	high

Fig.5. It is a parallel combination of two boost converter topology as shown in Fig.4 operating with 180 degree phase difference and this topology retains the advantage of both interleaving and bridgeless. By using interleaving topology, we can reduce the current ripples, voltage ripple, switching losses and suitable for high power applications.

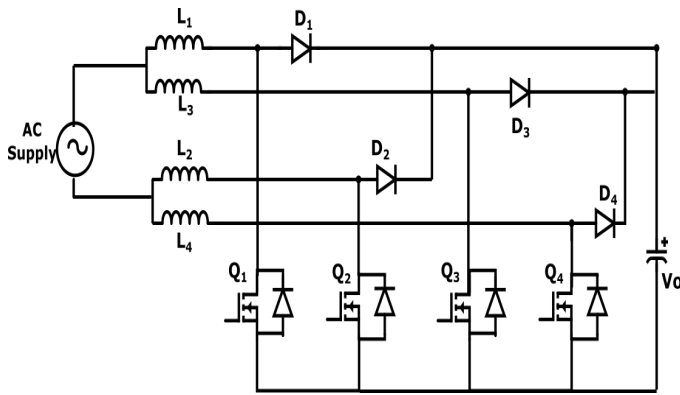Table II-D gives a comparison of proposed converter with

Fig. 5.   Bridgeless Interleaved boost converter

existing topologies. Even though so many advantages for bridgeless buck boost and bridgeless Luo converter, bridgeless boost converter is selected as PFC converter for proposed OBC for short distance low powered EVs because of its low cost, suitability for low applications and less number of switching devices. Hence the scheme proposed for OBC in EVs uses bridgeless boost PFC converter and is presented in the next session.

III. PROPOSED OBC WITH FRONT END BRIDGELESS BOOST PFC FOR EVs

In the proposed OBC scheme for short distance EVs uses front end PFC converter with a bridgeless boost converter topology and cascaded by second stage as LLC resonant DC-DC converter. Detailed design and selection of components are presented in the next section.

IV. DESIGN OF PROPOSED OBC FOR EV

The relation between output voltage, input voltage, power, duty cycle, operating frequency for the bridgeless boost converter stage and LLC converter stage are analysed through mathematical expressions and gain plots. First Harmonics Approximation (FHA) method is used here for the steady
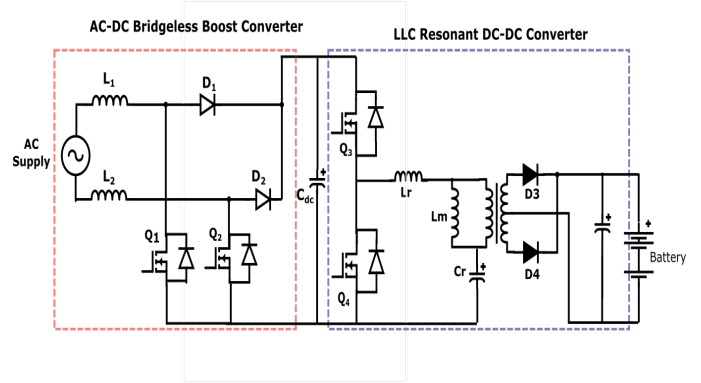

Fig. 6.   Proposed OBC with front end bridgeless boost PFC

state analysis of LLC stage . Since LLC converter operates near to series resonant frequency, FHA of input voltage gives accurate results.

A. Bridgeless Boost Converter

The front end dual boost converter is designed for a 500W load with an input single phase AC voltage of 230V and DC output of 400 V. By considering base voltage (Vbase)=230V, base power (Pbase)=500W and the frequency of ripple current as twice the input frequency, the value of capacitance C_{dc} for normalised switching frequency (n= fs/f) can be calculated using equation (1) and normalised inductive reactance value is designed using equation(2).

$$C_{dc} = \frac{I_o}{n\omega(\Delta V)} \quad (1)$$

$$X_{Ln} = \frac{V_{base}}{\Delta I_L} \quad (2)$$

where, $n = f_s/f$,
Table IV-A gives the designed parameters of front end AC-DC converter.

B. LLC Resonant converter

Square wave output from DC-DC converter is applied to the primary winding of the transformer and transferred to the secondary side of the transformer. Transformer turns ratio helps to deliver the required output voltage. The frequency at peak resonance f_c varies between the pole frequency f_p at no load and series resonant frequency f_0 when load terminals are under short circuit condition. Hence the impedance

TABLE II
PARAMETERS OF AC-DC CONVERTER

Parameters	symbol	Values
Current	I_{base}	2.17 A
ripple voltage	ΔV_L	5%
ripple current	ΔI_L	10%
Switching frequency	fs	20kHz
inductance	L	5.7 mH
capacitance	C_r	1300 μF

(a) Ln=1

(b) Ln=5

(c) Ln=10

(d) Ln=20

Fig. 8. LLC converter voltage gain function vs normalised switching frequency for different values of L_n and Q_e

variation of LLC converter follows a family of curves with $f_p \leq f_c \leq f_0$, instead of a single curve in series resonant circuit [14]-[17].

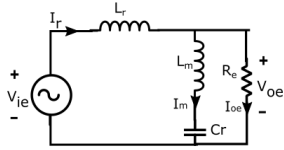As LLC converter mainly operates near series resonant

Fig. 7. Linear sinusoidal model of LLC converter

frequency, as an approximation the fundamental harmonic component alone can be considered for modeling of LLC resonant converter as shown in Fig.7

Voltage gain of the LLC converter, g_{LLC} is the ratio of output voltage to input voltage as in equation (3).

$$g_{LLC} = \frac{n \times V_o}{V_{in}/2} \qquad (3)$$

Normalised voltage gain can be written as,

$$g_{LLC} = \left| \frac{L_n \times f_n^2}{[(L_n+1) \times f_n^2 - 1] + j[(f_n^2 - 1) \times f_n \times L_n \times Q_e]} \right|$$

Where frequency as $f_n = \frac{f_s}{f_0}$, inductance ratio as $L_n = \frac{L_m}{L_r}$, and the quality factor Q_e as $\frac{\sqrt{L_r/C_r}}{R_e}$.

Output voltage V_o can be written as in equation (4)

$$V_o = g_{LLC} \times \frac{1}{n} \times \frac{V_{in}}{2} \qquad (4)$$

Fig.8 shows the variation of the gain of the LLC converter with normalised frequency for different values of Ln and Qe. It is clear that all the curves pass through the point (fn ,gLLC)=(1,1) which indicates that whatever be the load condition the value of gain remains unity at normalised frequency. Hence this operation point at (fn ,gLLC)=(1,1) or near to it helps to reduce the frequency variation to minimal range.To achieve better regulation in LLC converter the gain adjustment is done by modulating the switching frequency. The design is done for an input voltage of the range Vin-min of 375 V and Vin-max of 405 V, output voltage 48 V DC, rated output current(Io) 10.4 A, rated output power of 500 W , output voltage line and load regulation less than 1% and efficiency 90%. Transformer turn's ratio can be calculated for a nominal input voltage, V_{in-nom} of 390 V and a nominal output voltage, V_{o-nom}
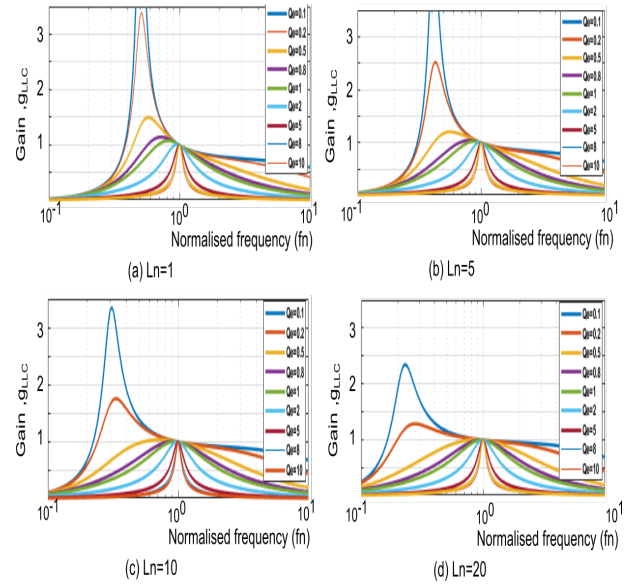
of 48 V using the equation(5)

$$n = g_{LLC} \times \frac{V_{in-nom}/2}{V_{o-nom}} \qquad (5)$$

Minimum and maximum values of gain are calculated using equation (6) and equation (7)as,

$$g_{LLC-min} = n \times \frac{V_{o-min} + V_F}{V_{in-max}/2} \qquad (6)$$

$$g_{LLC-max} = n \times \frac{V_{o-max} + V_F + V_{loss}}{V_{in-min}/2} \qquad (7)$$

To ensure soft switching ie, zero voltage switching the operation should be in inductive region,but the peak value lies in capacitive region.Hence the operating point and the value of L_n is to be chosen such as to avoid the capacitive region. From Figure9, it is clear that the range of variation of normalised frequency should be within the range of f_{nmin} and f_{nmax} to achieve the required output voltage regulation.

Resonant circuit constant L_r and C_r can be calculated using equations (8) and (9) by selecting the the switching frequency as 100 kHz initially same as series resonant frequency.

$$C_r = \frac{1}{2 \times \pi \times Q_e \times f_0 \times R_e} \qquad (8)$$

$$L_r = \frac{1}{(2 \times \pi \times f_0)^2 \times C_r} \qquad (9)$$

Where,

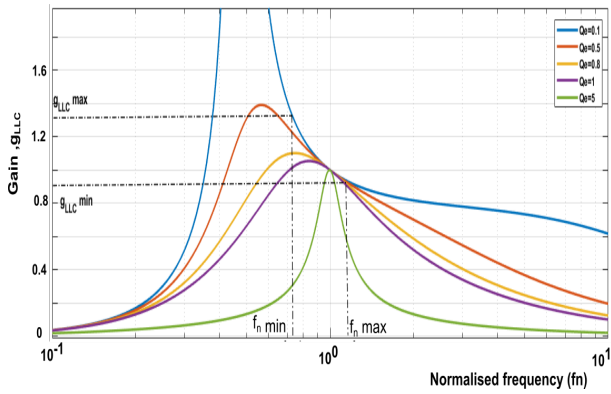$$R_e = \frac{8 \times n^2 \times R_L}{\pi^2}$$

Fig. 9. Gain plot for selection of switching frequency

Fig. 10. Input voltage and current waveform

The designed values of L_r and C_r are verified using the equation for series resonant frequency f_0 and quality factor Q_e. To ensure zero voltage switching , it has to operate in the inductive region. So that it should satisfy the conditions given by equation (10)

$$\frac{1}{2}(L_m + L_r)i^2_{m-peak} \geq \frac{1}{2}(2C_{eq})V^2_{in} \qquad (10)$$

For a MOSFET of $V_{ds} = 500V$ and $C_{ds} = 200pF$, condition for dead time between the switches t_d is calculated using equation (11) ,

$$t_d \geq 16C_{eq} \times f_{sw} \times L_m \qquad (11)$$

As the LLC converter is operating in ZVS region, switching losses are less which inturn improves the efficiency of converter under all load conditions. The designed values are tabulated in Table III.

Fig. 11. Input current waveform and its harmonic components

TABLE III
KEY PARAMETERS OF LLC RESONANT CONVERTER

Parameters	symbol	Rating
Power MOSFET	Q_2, Q_3	500V, 20 A
Power diodes	D_1, D_2	100V, 20 A
Inductance ratio	L_n	3.5
Magnetising inductance	L_m	157.5 μ H
Resonant inductance	L_r	45 μ H
Switching Frequency	f_s	70-105kHz
Resonant capacitance	C_r	59.124 nF
Dead time	t_d	100 ns
Transformer turns ratio	n	4
output capacitor		2000 μ F

V. SIMULATION RESULTS

The simulations are performed using MATLAB-Simulink for the designed values.Fig.10 shows the input current and voltage of front end Bridgeless boost converter. From the waveforms it is clear that current waveform is sinusoidal in nature and nearly in phase with voltage waveform.It is obtained a pf of 0.912. Fig.11 shows the Fourier spectrum of input current and which gives an idea about the harmonic content in the current waveform and it also compute the THD.
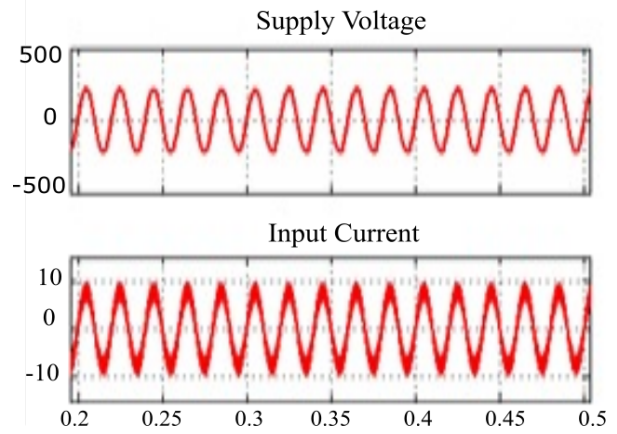

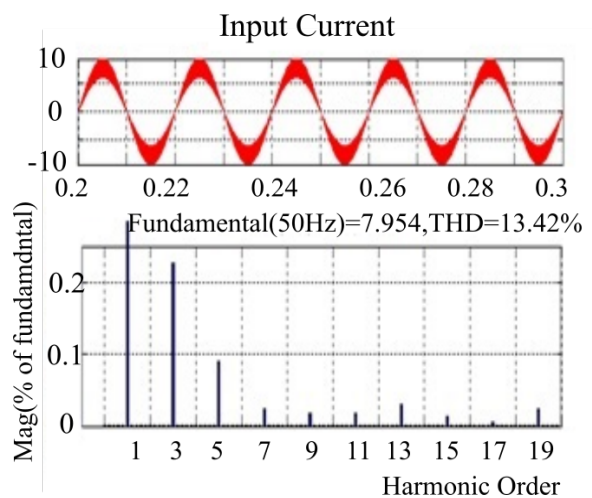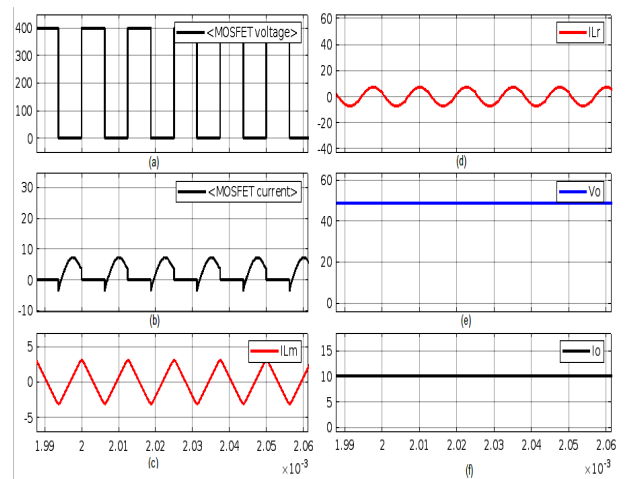Fig. 12. waveforms of LLC resonant converter(a) Voltage across MOSFET (b) current through MOSFET (c) Magnetising current of transformer (d) resonant current of LLC (e) output voltage (f)output current
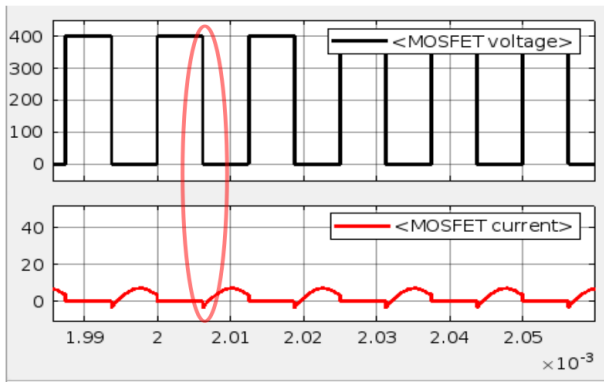
Fig. 13.   Waveforms of voltage across and current through MOSFET

During the charging mode of operation, single phase AC is converted into DC and this voltage is given as then input to LLC converter. The switching voltage and current waveforms of MOSFET, magnetizing current, resonant circuit current, output voltage across the capacitor and output current drawn by the battery during charging mode of operation in LLC resonant converter is given in Fig.12

From Fig.13, showing waveforms of the voltage across and current through switch Q2, it is clear that ZVS is attained resulting in reduced switching losses.

VI. CONCLUSIONS

The growing demand for electric vehicles warrants better performance of OBC circuits in terms of easiness of control, reliability, cost and less injection of harmonics into the system. The proposed scheme has focused on front end PFC used in OBC for batteries used in EVs. The bridgeless boost converter topology has minimum number of components and better input power factor. The proposed scheme is simulated on MATLAB- SIMULINK platform and from the results it is clear that a regulated DC output voltage is obtained for battery charging and OBC draws a current waveform of nearly sinusoidal. Considering the technological revolution occurring in the field of electric vehicle, an on board battery charger will be a boon to the future energy needs and hence the importance of the scheme proposed in this paper.

REFERENCES

[1] Sam CA, Jegathesan V. Bidirectional integrated on-board chargers for electric vehicles—a review. Sādhanā. 2021 Dec;46(1):1-4.
[2] Martinez R, Enjeti PN. A high-performance single-phase rectifier with input power factor correction. IEEE transactions on power electronics. 1996 Mar;11(2):311-317.
[3] Shreya, K., Srivastava, H., Kumar, P., Ramanathan, G., Madhavan, P. and Bharatiraja, C. CUK converter fed resonant LLC converter based electric bike fast charger for efficient CC/CV charging solution. Journal of Applied Science and Engineering. 24(3): 331-338.
[4] Wei W, Hongpeng L, Shigong J, Dianguo X. A novel bridgeless buck-boost PFC converter. IEEE Power Electronics Specialists Conference. 2008 Jun 15; 1304-1308.
[5] Zhao, B., Abramovitz, A. and Smedley, K., 2015. Family of bridgeless buck-boost PFC rectifiers. IEEE Transactions on Power Electronic., 30(12): 6524-6527.
[6] Deepa, M.U. and Bindu, G.R., 2016, December. Performance analysis of BLDC motor drive with power factor correction scheme. In 2016 IEEE International Conference on Power Electronics, Drives and Energy Systems (PEDES).2016. 1-5.
[7] Sayed, S.S. and Massoud, A.M., 2022. Review on state-of-the-art unidirectional non-isolated power factor correction converters for short-/long-distance electric vehicles. IEEE Access, 10;11308-11340.
[8] Xue L, Shen Z, Boroyevich D, Mattavelli P, Diaz D. Dual active bridge-based battery charger for plug-in hybrid electric vehicle with charging current containing low frequency ripple. IEEE Transactions on Power Electronics. 2015 Mar 16;30(12):7299-307.
[9] Pandey, R. and Singh, B., 2019. A power-factor-corrected LLC resonant converter for electric vehicle charger using Cuk converter. IEEE Transactions on Industry Applications. 55(6): 6278-6286.
[10] Zeng J, Zhang G, Yu SS, Zhang B, Zhang Y. LLC resonant converter topologies and industrial applications—A review. Chinese Journal of Electrical Engineering. 2020 Oct 6;6(3):73-84.
[11] Vu HN, Choi W. A novel dual full-bridge LLC resonant converter for CC and CV charges of batteries for electric vehicles. IEEE Transactions on Industrial Electronics. 2017 Aug 21;65(3):2212-25.
[12] Deshmukh S, Iqbal A, Islam S, Khan I, Marzband M, Rahman S, Al-Wahedi AM. Review on classification of resonant converters for electric vehicle application. Energy Reports. 2022 Nov 1;8:1091-113.
[13] Chen SY, Li ZR, Chen CL. Analysis and design of single-stage AC/DC LLC resonant converter. IEEE Transactions on Industrial Electronics. 2011 Aug 18;59(3):1538-44.
[14] Beiranvand R, Rashidian B, Zolghadri MR, Alavi SM. A design procedure for optimizing the LLC resonant converter as a wide output range voltage source. IEEE Transactions on Power Electronics. 2012 Feb 15;27(8):3749-63.
[15] Hu Z, Qiu Y, Liu YF, Sen PC. A control strategy and design method for interleaved LLC converters operating at variable switching frequency. IEEE Transactions on Power Electronics. 2014 Jan 14;29(8):4426-37.
[16] Qiu Y, Liu W, Fang P, Liu YF, Sen PC. A mathematical guideline for designing an AC-DC LLC converter with PFC. In2018 IEEE Applied Power Electronics Conference and Exposition (APEC) 2018 Mar 4 (pp. 2001-2008). IEEE.
[17] Huang H. Designing an LLC resonant half-bridge power converter. In 2010 Texas Instruments Power Supply Design Seminar. SEM1900, Topic 2010 Jul Vol. 3, 2010-2011.